



# ESTUDO DAS CARACTERÍSTICAS DO FLUXO DE GÁS ATRÁS DO QUEIMADOR DE VÓRTICE DA CÂMARA DE COMBUSTÃO DO MOTOR DE TURBINA A GÁS DE AERONAVES

## STUDY OF THE FEATURES OF GAS FLOW BEHIND THE VORTEX BURNER OF THE COMBUSTION CHAMBER OF AN AIRCRAFT GAS TURBINE ENGINE

### ИССЛЕДОВАНИЕ ОСОБЕННОСТЕЙ ТЕЧЕНИЯ ГАЗА ЗА ВИХРЕВОЙ ГОРЕЛКОЙ КАМЕРЫ СГОРАНИЯ АВИАЦИОННОГО ГАЗОТУРБИННОГО ДВИГАТЕЛЯ

RABINSKIY, Lev N.<sup>1\*</sup>; VAKHNEEV, Sergey N.<sup>2</sup>

<sup>1</sup> Moscow Aviation Institute (National Research University), Department of Advanced Materials and Technologies of Aerospace Application, 4 Volokolamskoe shosse, zip code 125993, Moscow – Russian Federation  
(phone: +7 499 158-40-43)

<sup>2</sup> Moscow Aviation Institute (National Research University), Department of Engineering Graphics, 4 Volokolamskoe shosse, zip code 125993, Moscow – Russian Federation  
(phone: +7 499 158-40-43)

\* Corresponding author  
e-mail: Rabinskiy@mail.ru

Received 21 June 2018; received in revised form 30 November 2018; accepted 04 December 2018

### RESUMO

Atualmente, os motores de turbina a gás são cada vez mais usados como usinas de energia no setor de energia, o setor de petróleo e gás, isto é, acontece o processo de conversão de turbinas a gás de aeronaves, que gastaram seus recursos de vôo, para turbinas a gás terrestres. Portanto, o estudo de processos na câmara de combustão de turbinas a gás de aeronaves é de particular relevância. Foi desenvolvida uma técnica para resolver analiticamente o cálculo das características geométricas e de ejeção de um fluxo dinâmico de gás na esteira dos queimadores de vórtice, que fornecem a preparação de uma mistura homogênea de ar-combustível nas câmaras de combustão de motores a jato de ar e outros dispositivos queimadores. É apresentado um modelo computacional de distribuição de fluxo de jatos coaxiais opostamente torcidos diretamente atrás do corte do queimador na zona de fluxo de circulação intensiva, onde o processo de combustão se estabiliza durante a combustão do combustível. As condições são mostradas sob as quais é possível avaliar a estabilidade da combustão de uma mistura homogênea no estágio de projeto dos dispositivos de vórtice.

**Palavras-chave:** câmara de combustão, queimador de vórtice, jatos torcidos, zona de circulação, estabilização de combustão.

### ABSTRACT

Currently, gas turbine engines are increasingly used as power units in the power industry, oil and gas industries, i.e., the process of converting aircraft gas turbine engines that have exhausted their flying resource into gas turbine installations for surface applications is underway. Therefore, the study of processes in the combustion chamber of aircraft gas turbine engines becomes particularly urgent. An analytical method for calculating the geometric and ejection characteristics of the gas-dynamic flow in the wake of the vortex burners is developed, which ensures the preparation of a homogeneous fuel-air mixture in the combustion chambers of air-jet engines and in other burner devices. The calculated model of the flow of coaxial, opposite swirling jets directly behind the cut of the burner in the zone of intensive circulation flow, where the combustion process

stabilizes. The conditions under which it is possible to estimate the stability of combustion of a homogeneous mixture at the stage of design of vortex devices are shown.

**Keywords:** *combustion chamber, vortex burner, swirling jets, circulation zone, combustion stabilization.*

## АННОТАЦИЯ

В настоящее время газотурбинные двигатели находят всё более широкое применение в качестве силовых установок в энергетике, нефтяной и газовой промышленности, то есть происходит процесс конвертирования авиационных газотурбинных двигателей, отработавших свой летный ресурс, в газотурбинные установки наземного применения. Поэтому исследование процессов в камере сгорания авиационных газотурбинных двигателей приобретает особую актуальность. Разработана методика аналитического решения расчета геометрических и эжекционных характеристик газодинамического потока в следе за вихревыми горелками, обеспечивающими подготовку гомогенной топливо-воздушной смеси в камерах сгорания воздушно-реактивных двигателей и в других горелочных устройствах. Приведена расчетная модель распространения потока соосных противоположно закрученных струй непосредственно за срезом горелки в зоне интенсивного циркуляционного течения, где при сжигании топлива происходит стабилизация процесса горения. Показаны условия, при которых возможна оценка устойчивости горения гомогенной смеси на стадии проектирования вихревых устройств.

**Ключевые слова:** *камера сгорания, вихревая горелка, закрученные струи, циркуляционная зона стабилизация горения.*

## INTRODUCTION

On the basis of aircraft air-jet engines, it is rather advantageous to produce gas-turbine installations, since in this case, the costly materials used in their production offer savings, which allows saving about 70-75% of the major units and components of the basic engine. In addition, the conversion of aircraft engines is associated with the geography of the location of natural resources on the territory of the Russian Federation, which is concentrated mainly in the eastern regions of Western and Eastern Siberia, while the main energy consumers are in the European part of the country and in the Urals (Budiman and Zuas, 2015). In this case, it is possible to organize the transportation of energy resources from east to west by cheap, transportable engine installations of optimal power with a high level of automation. In this regard, the trouble-free performance of air-jet engines and, first and foremost, the stable operation of the combustion chamber, becomes of particular urgency (Formalev *et al.*, 2016; Bulychev *et al.*, 2018).

In modern combustion chambers of an air-jet engine, vortex burners are used to meet rigid ecological, economic and special requirements for the preparation and combustion of fuel-air mixtures. The stability of the combustion chamber depends significantly on the organization of the combustion process of fuel-air mixture behind the burner: distribution of gas-dynamic parameters in

the flow, mass transfer in the circulation zone, and flow geometry. The estimation of combustion stability boundaries in the combustion chamber, especially when the mixture is lean, an individual burner and, as a consequence, the entire combustion chamber, allows to significantly shorten the terms of the design stage of the product, to design combustion chambers purposefully at specified parameters.

## METHODOLOGY

The technique of the analytical decision on the definition of volume of a circulation zone and mass transfer in it, an aerodynamic trace behind a vortex burner is further presented. The burner diagram and the gas flow are shown in Figure 1.

The burner consists of two coaxial vane swirlers, one of which (T3) is supplied with air and fuel by a jet nozzle, the other (V3) is supplied with air. Two oppositely swirled jets in a common cut (cross-section 0-0) form a single swirling jet, which then spreads along the exhaust stack of the burner and, after cross-section 1-1, – in free space. In the wake of the burner, a developed circulation zone arises, the dimensions of which are determined by the swirling parameters of individual swirlers and the geometry of the exhaust stack.

The flow behind the burner is typical for the flow of strongly swirled jets: a circular swirling jet

with axial and circumferential components of the general speed vector, intense near-axis reverse current, uniform temperature distribution over the cross-section of the circulation zone and a high level of flow turbulence (Shchukin and Khalatov, 1982).

The calculation is based on consideration of the regularities of the propagation of an annular swirling jet formed when the air from the burner is exhausted and its mass exchange with the surrounding medium (Abramovich, 1974; Akhmedov, 1974; Uryvsky, 1982; Belousov and Knysh, 1977). It is assumed that:

- 1) The mixture leaving the fuel-air swirler is homogeneous;
- 2) The flow parameters (speed, composition, temperature) in the cross-section of the jet are uniform;
- 3) Gas parameters (temperature, air excess coefficient  $\alpha$ ) are constant throughout the volume of the circulation zone and are equal to the parameters in cross-section 2, and the fuel combustion completeness is  $\sim 0,85$ ;
- 4) The gas flow through the circulation zone is equal to the flow rate of the ejected jet from the near-axis area;
- 5) In the entire flow field, the axial impulse and the angular momentum of the jet remain unchanged.

## RESULTS AND DISCUSSION:

The calculation task is to determine the ejection of the mass in the jet from the near-axis area and the surrounding medium, and also to find the trajectory of the jet in free space. On the basis of these quantities, it is possible to determine the volume of the circulation zone, the composition of the mixture in it, and the flow through it, which will allow us to estimate the value  $\frac{G_B}{V_p \bar{P}^2}$  and  $\alpha_{max}$  behind a vortex burner (Tsyganov, 2007; Lansky *et al.*, Bortnikov, 1976; Volkov, 2000; Gorbunov, 1972; Knysh, 1982; Lansky, 1998; Lefevre, 1986; Sudarev and Maev, 1990).

The points in the vortex burner can be divided into 2 sections: I – from the fuel-air swirler to the mixing of jets (cross-section 0-0) and the flow of the combined jet inside the exhaust stack of the burner (cross-section 1-1); II – jet propagation outside the burner (Figure 1)

(Vakhneev *et al.*, 2016).

The flow in section 1 to cross-section 0-0 is formed by a fuel-air swirler with a swirl parameter  $S_{T3}$ . The propagation of a swirling jet occurs in a cylindrical channel of radius  $\bar{r}_{T3}$  of the swirl chamber of the swirler. Axis of jet  $\bar{z}$  is directed along the channel wall. The axial impulse of such a jet with respect to the averaged parameters is equal to Equation 1 but the angular momentum Equation 2. Where  $\varphi$  – coefficient of the jet cross-section,  $G$  – air flow through the swirler;  $F_{\varphi}$  – the area of the swirl chamber;  $F_{\varphi}$  – the area occupied by the jet;  $l$  – swirling arm of the swirler. Inside the annular jet, there is a near-axis reverse gas flow with maximum radii of  $r_{\varphi}$ . The area occupied by the jet (the relative thickness of the jet  $\bar{b}_{T3}$ ) was determined by calculating the filling factor of the cross-section  $\varphi_{T3}$  with the use of the dependence  $\varphi = f(S)$ , obtained for the case of fluid outflow (Abramovich, 1991). As the flow progresses, a mass of gas is ejected from the near-axis area into the swirling jet. To calculate the ejection capacity of the jet, the results of studies of coflowing turbulent gas jets are used (Vakhneev *et al.*, 2016; Lukachev and Tsyganov, 2004; Lansky *et al.*, 1998; Ivliev *et al.*, 1986; Lukachev *et al.*, 1998).

Considering the section I of the jet propagation as the initial one for some turbulent semibounded jet, we use the following dependency (Equation 3). Ejection of mass in a jet of width  $b_{T3}$  in the initial section of length  $z$ , equal to the longitudinal dimension of the swirl chamber, is carried out from the zone of reverse currents with density  $\rho_u$  and temperature  $T_u$ . Coefficient value  $C_1$  for flooded jets is 0.0362. The relative increase in mass per unit length of the section  $dz$  (Equation 4) or approximately for a section of a jet of length  $\Delta z$  in finite differences (Equation 5). Since the suction of the mass in the jet will generally change with a change in its surface, it is natural to assume that the ejection of the mass additionally varies in proportion to the radius of the jet. The swirl of the flow increases its ejection ability. Suppose that the swirl of the flow increases the ejection of mass into the jet due to an increase in its total amount of motion compared to the axial amount of motion. Then it is natural to assume that the suction of the mass increases in proportion to the ratio of the total velocity vector  $V$  to the axial  $U_z$ . Then the value of the weight gain, taking into account the above, will be Equation 6. Replacing the relationship  $\frac{V}{U_z}$

through the parameter of the jet, passing to relative values and taking into account that  $\frac{\rho_0}{\rho} = \frac{1}{\bar{T}_u}$ , and  $\bar{b} = 1 - \sqrt{1 - \varphi_{T3}}$ , after some transformations we obtain a relationship connecting the increase in mass on the elementary length  $\Delta\bar{z}$  with flow parameters (Equation 7). Where  $K_{M_i}$  – coefficient that takes into account the change in the angular momentum of the jet due to ejection of mass into it;  $\bar{r}_\varphi$  – radius of the boundary of the jet, over which mass exchange takes place with the near-axis area. Here, the coefficient  $\frac{1}{2}$  takes into account the unilateral ejection of the mass into the jet.

Due to the ejection of the mass into the annular jet of the fuel-air mixture from the near-axis region of the reverse flow, its angular momentum will vary in proportion to the attached one –  $G_{\text{EII}}$ . In an unspecified cross-section of the jet, the angular momentum  $M_i$  is proportional to the original moment behind the swirl M and the coefficient  $K_M$ , which depends on the ejection of the mass in the jet, i.e. (Equation 8), where (Equation 9). The flow at the common cut of the burner is formed as a result of the interaction of two oppositely swirled jets. It is assumed that an instantaneous mixing of air and mixture flow takes place in cross-section O-O (Figure 1), and the resulting annular swirling jet then propagates. The angular momentum of such a jet is equal to the difference in the angular momentum of the individual flows in cross-section O-O (Equation 10). The axial impulse is defined as the sum of the axial impulses of individual jets (based on the averaged parameters) (Equation 11), where  $\rho_0$  – the resultant jet density;  $G_{\text{EII}}$  – mass ejected into the jet in section I. The coefficient of the cross-section of the resulting jet (Equation 12). The conditional swirl parameter of the jet formed is Equation 13 or through the main flow parameters (Equation 14). Due to the intensive mixing of the jets of individual swirlers above the cross-section O-O, the flow can be considered as the main section of the turbulent semibounded jet. Introducing, similarly to section I, the assumptions about the proportionality of the mass suction by the quantities  $r/r_0$  and  $/U_z$ , after some transformations we obtain the formula for calculating the ejection capacity of the jet in the section under consideration (Equation 15).

Since a number of simplifying assumptions were adopted in the course of calculation of the jet in this section (for example, the assumption of

instant mixing of jets formed by the burner swirls), in form (12), an empirical constant  $K_u$  was introduced for the ejection of the mass from the reverse current zone. The value  $K_u = 3,0 \div 3,2$  was calculated based on the results of the determination of the flow in the forward and reverse currents at the burner cut with cold products and was kept constant in all subsequent calculations. In this case, the increased values of the coefficient  $K_u$  is determined by the high intensity of the mixing processes in the zone of interaction of the jet with the reverse current.

The trajectory of the jet in the burner is determined, basically, by the shape of the exhaust stack  $\bar{z} = f(\bar{x})$ . The basis of its calculation is the determination of the jet thickness (taking into account the ejecting gas mass) during flow along the generatrix of the exhaust stack.

In section 2, the jet propagates in free space. With regard to the above mentioned, ejection of mass into the jet occurs both from the near-axis area and from the surrounding space. The value of the attached mass from the return flow zone is calculated in the same way as in section I, and from the surrounding space, taking into account its temperature, according to the following Equation 16.

Coefficient value  $K_H$  according to the results of the calculations, is equal to 1, since the interaction of the external surface of the jet occurs with unperturbed flooded space.

The flow of a jet in a closed area occurs under the action of pressure drop  $\Delta P = P_H - P_u$  between the environment and the circulation zone, which curves the trajectory and leads to a "compression" of the jet. For an approximate determination of the value  $\Delta P$  the Equation of momentum conservation for the circuit is used (Figure 2). In accordance with Euler's theorem on momentum, the force acting in the direction of the x-axis on the selected contour is equal to the change in the axial impulse of the second gas flow through the circuit (Equation 17), where  $J_{06p1}$  – the main impulse of the reverse flow into cross-section 1;  $J_{np1}$  – the axial impulse of the jet in cross-section 1;  $J_3$  – axial momentum in the jet in cross-section 3, where  $P_3 \cong P_H$ . It is assumed that in this cross-section the axial impulse of the jet decreases in proportion to the removal of a part of the mass into the reverse current, i.e. (Equation 18), where Equation 19. For a constant density, the value  $K \sim 0,5$  [1]. From Equation 14,

after transformation, a relationship can be obtained to determine the relative pressure difference between the surrounding space and the circulation zone (Equations 20, 21), where the relative flow in the jet in cross-section Equation 22, where  $\bar{T}_1$  – relative temperature in cross-section 1;  $\bar{r}_K$  – the relative radius of the exhaust stack. The outlet angle of the jet from the burner exhaust stack in cross-section 1.  $\cos(\text{Equation 23})$ . In the field of pressure forces ( $\Delta\bar{P}$ ) and the inertia arising from the swirl of the flow, the jet trajectory is formed. To calculate it, we use the Equation of motion for the elementary  $\Delta m$  jet in the projection on the axis OY (see Figure 2). External forces acting on the element  $\Delta m$  is represented by the pressure force  $N_p$ , and the vector of total acceleration is equal to the sum of the vectors of relative and absolute motions (Equation 24), where  $\Delta\gamma$  – angular size of the selected element;  $\chi$  – angle between the vectors of relative and absolute acceleration at point O; R – radius of curvature of the trajectory at the point under consideration; r – current radius of the annular jet. Equation (17) can be reduced to the form Equation 25 and is a nonlinear differential equation of the second order that connects the coordinates of the jet in an open space with the flow conditions.

Thus, for the entire flow behind the vortex burner from the jet exit from the swirlers to the end of the circulation zone, the trajectory of the jet and the ejection of the mass into it can be calculated. For the end of the circulation zone, a certain cross-section 2 is taken, where the axis of the jet has an inflection point (Figure 1).

The calculation is carried out by the method of successive approximations when the jet is divided into a sufficiently small step size  $\Delta\bar{x} = 0,01$ , further reduction of which does not lead to an increase in the accuracy of calculations.

In this case, differential flow equations are replaced by finite-difference equations.

Equation 17 is solved with respect to the radius of curvature  $\bar{R}$  Equation 26 and within the limits of the partition step, the trajectory of the jet is approximately represented by an arc of a circle of radius  $\bar{R}$ . In the first approximation ( $j=0$ ), the value of the mass ejection from the surrounding space  $\bar{G}_{\text{3H}_0} = 0,5$ . For each elementary section  $\Delta\bar{x}$  the ejection of mass from the surrounding space is determined  $\Delta\bar{G}_{\text{3H}_i}$ ; the near-axis area  $\bar{G}_{\text{3H}_i}$  and the elementary volume  $\Delta\bar{V}_i$ . The calculation is carried out to cross-section 2, where the

trajectory of the jet has an inflection point and  $\frac{1}{\bar{R}} \rightarrow 0$ . In the first approximation, the length of the circulation zone is taken as the distance  $\bar{x}_2$ , where the curvature of the trajectory tends to 0. After calculating the flow to  $\bar{x}_2$  the total values  $\bar{G}_{\text{3H}_j} = \sum_{i=1}^n \Delta\bar{G}_{\text{3H}_i}$ , characterizing the composition of the mixture in the circulation zone,  $\bar{G}_{\text{3H}_j} = \sum_{i=1}^n \Delta\bar{G}_{\text{3H}_i}$ ,  $\bar{V}_j = \sum_{i=1}^n \Delta\bar{V}_i$  and the value  $\bar{G}_{\text{3H}_j}$  is compared with the given ( $j-1$ ). In the next cycle of calculation for the value  $\bar{G}_{\text{3H}}$  its found value is accepted. And so until the conditions are met Equation 27, where  $\varepsilon$  – the required accuracy of the calculation is 0.01.

Thus, as a result of the calculation of the flow structure, the values of the ejected masses from the reversed flow area  $\bar{G}_{\text{3H}}$  can be obtained and from the surrounding space  $\bar{G}_{\text{3H}}$ , as well as the volume of the circulation zone  $\bar{V}_j$ , determined by the trajectory of the jet, and the composition of the gas in it  $\alpha_{\text{H}}$ .

According to the above procedure, calculations of the jet axis trajectory were made and compared with the experimental results with cold blows. In Figure 3, the calculated trajectory of the jets is shown by a solid line for two forms of the exhaust stack.

The experimental points of the axis of the direct current jet were taken from the maximum values of the axial impact air pressure in the corresponding cross-sections. As we can see, on the whole, the agreement between calculation and experiment can be considered satisfactory. The longitudinal dimensions of the circulation zone determined experimentally are also close to the calculated ones:  $\bar{x}_2 = \bar{x}_{\text{H}}$  calculation for burners without an annular nozzle is within the range of 6.0÷7.0 (for the burners studied), and with the annular nozzle – 4.0÷5.0; and  $\bar{x}_{\text{H}}$  – experimental is 6,5÷7,5, and 4,0÷6,0, respectively.

## CONCLUSIONS:

Thus, it can be concluded that the proposed scheme of the flow structure and the calculation method based on it satisfactorily describe the main features of the flow in vortex-type burners and can be used for approximate calculations of the stall characteristics of vortex burners. Based on these studies it is possible to modernize the combustion chamber of converted aircraft gas turbine engines. This will ensure a

fuel burn-out process in which the gas temperature distribution along the length of the can-type combustion chamber has the minimum values of local gas temperatures. In the future, the decrease in residence time of the combustion products in the combustion chamber is possible, and for this purpose, it is installed in the front device of the burners with a reducing nozzle. In this case, the gradient of the transverse speed of the outflowing mixture is maximal, which ensures a complete burnout of the fuel at a short length, as a result of which the combustion chamber can be reduced in size. This problem is described in detail in.

## REFERENCES

1. Abramovich, G.N. *Applied gas dynamics*, Moscow: Nauka, 1991.
2. Abramovich, G.N. *Turbulent tracking of gas jets*, Moscow: Nauka, 1974.
3. Akhmedov, R.B. *Aerodynamics of a swirling jet*, Moscow: Energiya, 1977.
4. Belousov, A.N., Knysh, Yu.A. *The use of vortex burners in aviation gas turbines for surface use. Ground application of aircraft engines in the national economy*, Moscow: VIMI, 1977.
5. Bortnikov, M.T. *Proceedings of CIAM*, 1976, 613, 63.
6. Budiman, H.; Zuas, O. *Periodico Tche Quimica*, 2015, 12(24), 7-16.
7. Bulychev, N.A., Kuznetsova, E.L., Bodryshev, V.V., Rabinskiy, L.N. *International Journal of Nanomechanics Science and Technology*, 2018, 9(2), 91-97
8. Formalev, V.F., Kolesnik, S.A., Kuznetsova, E.L., Rabinskii, L.N. *High Temperature*, 2016, 54(3), 390-396.
9. Gorbunov, G.M. *Selection of parameters and calculation of the main combustion chambers GTE*, Moscow: MAI, 1972.
10. Ivliev, A.V., Postnikov, A.M., Rozo, V.G., Savchenko, V.P., Tsyganov, A.M. *Influence of the angle of blade installation on the characteristics of vortex burners. Design and development of aviation gas turbine engines*, Kuibyshev: KuAl, 1986.
11. Knysh, Yu.A. *Burning in the Stream. Intercollegiate Collection*, 1982, 3, 27-31
12. Lansky, A.M. *Bulletin of SSAU. Series: Combustion Processes of Heat Exchange and Ecology of Thermal Engines*, 1998, 1, 228-240
13. Lansky, A.M., Matveyev, S.G., Lukachev, S.V. *Working process of combustion chambers of small-size GTE*, Samara: SSC RAS, 2009.
14. Lansky, A.M., Tsyganov, A.M., Fetisov, V.I., Shamban, M.A. *Bulletin of SSAU. Series: Combustion, Heat Transfer and Ecology of Thermal Engines*, 1998, 14, 240-246.
15. Lefevre, A. *Processes in combustion chambers GTE*, Moscow: Mir, 1986.
16. Lukachev, S.V., Lansky, A.M., Abrashkin, V.Yu., Didenko, A.A., Zubkov, P.G., Kovyllov, Yu.L., Matveev, S.G., Tsyganov, A.M., Shamban, M.A., Yakovlev, V.A. *Bulletin of SSAU. Series: Processes of Combustion, Heat Transfer and Ecology of Thermal Engines*, 1998, 1, 11-39.
17. Lukachev, S.V., Tsyganov, A.M. *Bulletin of SSAU. Series Processes of combustion, heat transfer and ecology of thermal engines*, 2004, 5, 223-226.
18. Shchukin, V.K., Khalatov, A.A. *Heat transfer, mass transfer and hydrodynamics of swirled flows in axisymmetric channels*, Moscow: Mashinostroyeniye, 1982.
19. Sudarev, A.B., Maev, V.A. *Combustion chambers of gas turbine installations. Intensification of combustion*, Leningrad: Nedra, 1990.
20. Tsyganov, A.M. *Bulletin of SSAU*, 2007, 2(13), 191-195.
21. Uryvsky, AF *Research of non-stationary modes of operation of vortex torches of aviation gas turbine engines*, Kazan: KAI, 1982.
22. Vakhneev, S.N., Korzhov, N.P., Kravchik, T.N. *Izvestiya of Tula State University, engineering sciences*, 2016, 1, 112-120.
23. Volkov, S.A. *Bulletin of SSAU. Series: Combustion Processes of Heat Exchange and Ecology of Thermal Engines*, 2000, 3, 20-24.

$$J = 2\pi\rho \int_r^{r_\phi} r(P + \rho U^2) dr = \frac{G}{\rho F_\phi}. \quad (1)$$

$$M = 2\pi\rho \int_r^{r_\phi} r^2 W U dr = \frac{Gl}{\rho \mu F_{ex}} \quad (2)$$

$$\bar{G} = \frac{G}{G_0} = C_1 \sqrt{\frac{\rho_i}{\rho}} \cdot \left( \frac{z}{b} + 1 \right) \quad (3)$$

$$\frac{d\bar{G}}{dz} = \frac{C_1}{b} \cdot \sqrt{\frac{\rho_i}{\rho}} \quad (4)$$

$$\Delta \bar{G} = \frac{\Delta G}{G_0} = C_1 \frac{\Delta z}{b} \sqrt{\frac{\rho_i}{\rho}} \quad (5)$$

$$\Delta \bar{G} = C_1 \sqrt{\frac{\rho_i}{\rho}} \cdot \frac{\Delta z}{b} \cdot \frac{r}{r_{T3}} \cdot \frac{V}{U_z} \quad (6)$$

$$\Delta \bar{G}_{II} = \frac{C_1 \cdot \Delta \bar{z}}{2(1 - \sqrt{1 - \varphi_{T3}})} \cdot \sqrt{\frac{(K_{Mi} \varphi_{T3} S_{T3})^2 + \bar{r}_\varphi^2}{\bar{T}_i}} \quad (7)$$

$$M_i = K_{M_i} \cdot M, \quad (8)$$

$$K_{M_i} = 1 + \frac{\bar{G}_{III_i}}{1 + \bar{G}_{III_H}} \quad (9)$$

$$M_0 = |K_M M_{T3} - M_{B3}| \quad (10)$$

$$J_0 = J_{T3} + J_{B3} = \frac{(G_{T3} + G_{B3} + G_{III})^2}{\rho_0 F_{B3} \varphi} = \left( \frac{G_0 + G_{III}}{\rho_0 F_{B3} \varphi} \right)^2 \quad (11)$$

$$\varphi = \frac{F_{B3} \varphi_{B3} + F_{T3} \varphi_{T3}}{F_{B3}} \quad (12)$$

$$S_0 = \frac{M_0}{J_0 r_0} = \frac{|M_{T3} K_M - M_{B3}|}{J_0 r_{T3}} \quad (13)$$

$$\Delta \bar{G}_{II_i} = K_i \cdot \frac{C_2 \Delta \bar{Z}}{4} \cdot \sqrt{\frac{(K_{Mi} S_0)^2 + \bar{r}_i^2}{\bar{T}_i (1 - \sqrt{1 - \varphi} \cdot \bar{Z})}} \quad (15)$$

$$\Delta \bar{G}_{III_{H_i}} = \Delta \bar{G}_{III_{H_i}} \cdot \frac{K_H}{K_i} \cdot \sqrt{\frac{\bar{T}_i}{\bar{T}_H}} \quad (16)$$

$$-(P_H - P_i) F_K = (J_3 - J_{06p1}) - J_{np1} \cos \beta \quad (17)$$

$$J_3 = J_2 = J_0 K, \quad (18)$$

$$K = \frac{G_2 - G_{06p}}{G_2} \quad (19)$$

$$\Delta \bar{P} = \frac{\Delta P}{\rho_0 U_0^2} \cdot \frac{1}{2} \quad (20)$$

$$\Delta \bar{P} = \frac{\varphi}{\bar{r}_K^2} \left[ \cos \beta - K + \left( \frac{1 - \bar{G}}{\bar{G}} \right)^2 \cdot \frac{\bar{T}_u}{\bar{T}_1} \cdot \frac{1}{\left( \frac{\bar{r}_K^2}{\varphi \bar{G}^2 \bar{T}_1} - \cos \beta \right)} \right] \quad (21)$$

$$1 \bar{G} = \frac{G_{np1}}{G_0} = \bar{G}_{\Theta H_1} + 1. \quad (22)$$

$$\beta = \frac{1}{\sqrt{1 + \left( \frac{d\bar{r}_1}{d\bar{x}_1} \right)^2}} \quad (23)$$

$$\Delta P \cdot \Delta z \cdot z \cdot \Delta \gamma = \Delta m \left( \frac{U_z^2}{R} + \frac{W^2}{r} \cos \chi \right) \quad (24)$$

$$2\Delta \bar{P} \left( \frac{\bar{r}}{\varphi} \right) = \left\{ \frac{\frac{d^2 \bar{r}}{d\bar{x}^2}}{\left[ 1 + \left( \frac{d\bar{z}}{d\bar{x}} \right)^2 \right]^{3/2}} + \frac{S_0^2 \left( \frac{dK_M}{d\bar{x}} \right)^2}{\bar{r}^3 \sqrt{1 + \left( \frac{d\bar{r}}{d\bar{x}} \right)^2}} \right\} \quad (25)$$

$$\bar{R} = \frac{1}{2\Delta \bar{P} \frac{\bar{r}}{\varphi} - (K_M S_0)^2 \frac{\cos \chi}{\bar{r}^3}} \quad (26)$$

$$\left| \bar{G}_{\Theta H_{j-1}} - \bar{G}_{\Theta H_j} \right| \leq \varepsilon \quad (27)$$

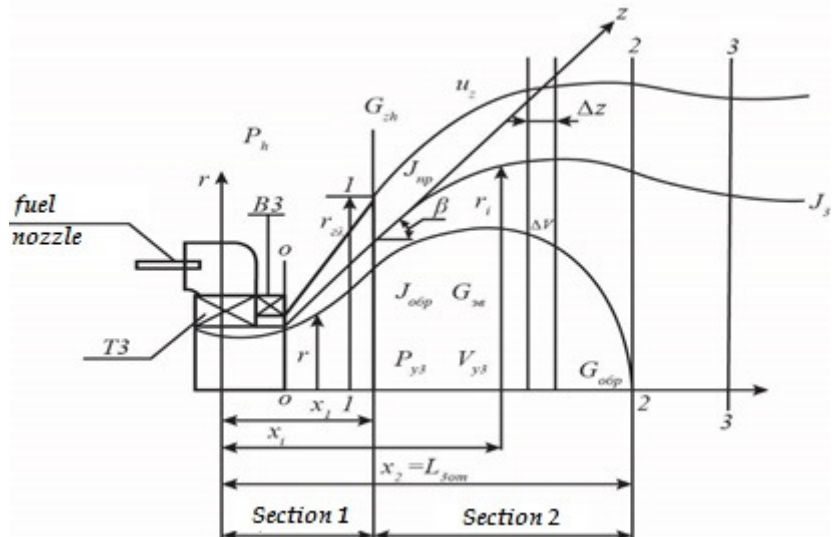


**Figure 1.** Burner and gas flow diagram

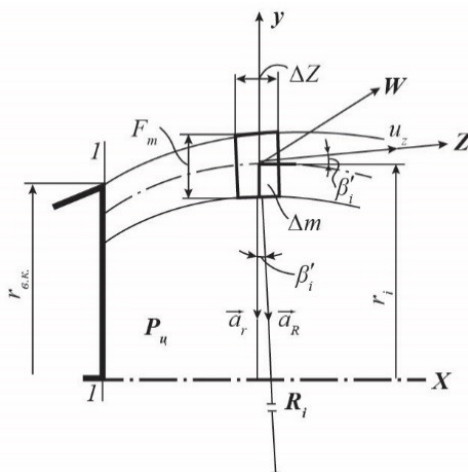


**Figure 2.** Design circuit for determining the pressure difference

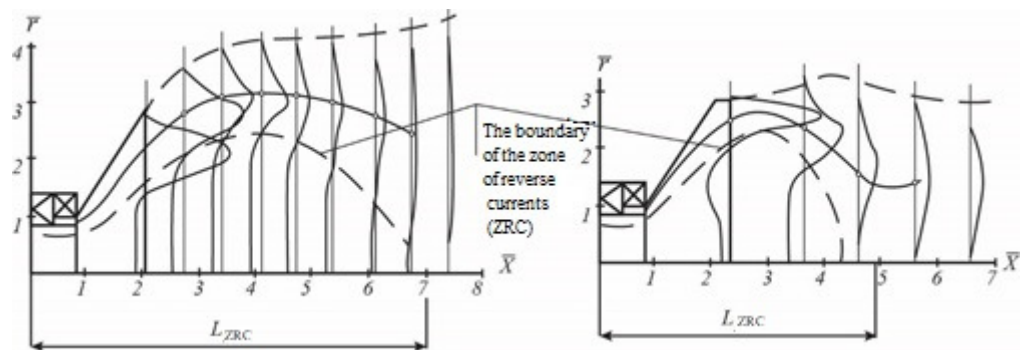


**Figure 3.** The calculated trajectory of jets for two types of the exhaust stack